

# Associations between organophosphorus pesticides exposure and age-related macular degeneration risk in U.S. adults: analysis from interpretable machine learning approaches

Yu-Xin Jiang<sup>1,2,3,4</sup>, Si-Yu Gui<sup>1,2,3,4</sup>, Xiao-Dong Sun<sup>1,2,3,4</sup>

<sup>1</sup>Department of Ophthalmology, Shanghai General Hospital, Shanghai Jiao Tong University School of Medicine, Shanghai 200080, China

<sup>2</sup>National Clinical Research Center for Eye Diseases, Shanghai 200080, China

<sup>3</sup>Shanghai Key Laboratory of Fundus Diseases, Shanghai 200080, China

<sup>4</sup>Shanghai Engineering Center for Visual Science and Photomedicine, Shanghai 200080, China

**Correspondence to:** Xiao-Dong Sun and Si-Yu Gui. Department of Ophthalmology, Shanghai General Hospital, Shanghai Jiao Tong University School of Medicine, 100 Haining Road, Shanghai 200080, China. xdsun@sjtu.edu.cn; whisperme@sjtu.edu.cn

Received: 2025-02-23 Accepted: 2025-04-21

## Abstract

• **AIM:** To investigate the associations between urinary dialkyl phosphate (DAP) metabolites of organophosphorus pesticides (OPPs) exposure and age-related macular degeneration (AMD) risk.

• **METHODS:** Participants were drawn from the National Health and Nutrition Examination Survey (NHANES) between 2005 and 2008. Urinary DAP metabolites were used to construct a machine learning (ML) model for AMD prediction. Several interpretability pipelines, including permutation feature importance (PFI), partial dependence plot (PDP), and SHapley Additive exPlanations (SHAP) analyses were employed to analyze the influence from exposure features to prediction outcomes.

• **RESULTS:** A total of 1845 participants were included and 137 were diagnosed with AMD. Receiver operating characteristic curve (ROC) analysis evaluated Random Forests (RF) as the best ML model with its optimal predictive performance among eleven models. PFI and SHAP analyses illustrated that DAP metabolites were of significant contribution weights in AMD risk prediction, higher than most of the socio-demographic covariates. Shapley values

and waterfall plots of randomly selected AMD individuals emphasized the predictive capacity of ML with high accuracy and sensitivity in each case. The relationships and interactions visualized by graphical plots and supported by statistical measures demonstrated the indispensable impacts from six DAP metabolites to the prediction of AMD risk.

• **CONCLUSION:** Urinary DAP metabolites of OPPs exposure are associated with AMD risk and ML algorithms show the excellent generalizability and differentiability in the course of AMD risk prediction.

• **KEYWORDS:** age-related macular degeneration; organophosphorus pesticide; National Health and Nutrition Examination Survey; interpretable machine learning; prediction

**DOI:10.18240/ijo.2025.07.04**

**Citation:** Jiang YX, Gui SY, Sun XD. Associations between organophosphorus pesticides exposure and age-related macular degeneration risk in U.S. adults: analysis from interpretable machine learning approaches. *Int J Ophthalmol* 2025;18(7):1214-1230

## INTRODUCTION

Age-related macular degeneration (AMD) is the leading cause of severe vision impairment in the elderly and is anticipated to influence approximately 288 million individuals worldwide by 2040<sup>[1-2]</sup>, placing a tremendous burden on both individuals and society. Currently, AMD is recognized as a multifactorial disease caused by number of risk factors such as aging, genetic susceptibility, lifestyle habits, and environmental exposures, which make the pathogenesis of AMD highly intractable to predict and interpretate. Intravitreal injection of anti-vascular endothelial growth factor (anti-VEGF) agents is the first-line therapy for exudative neovascular AMD<sup>[2]</sup>, but responses of patients vary. However, the shortcomings of the prevailing delivery method, characterized by low patient compliance, substantial financial expenses, and complications, such as eye pain, endophthalmitis, and lens injury, have

become increasingly apparent over time<sup>[3]</sup>. Therefore, early prevention of AMD from exposure to numerous risk factors is the most effective and feasible measure. Among all the factors, the adverse effects from environmental chemical exposures on AMD have been heated discussed in the field of population-based epidemiological studies. For example, several researches have emphasized the impacts of heavy metals<sup>[4]</sup>, air pollutants<sup>[5]</sup>, and radiation<sup>[6]</sup> exposure on the development of AMD.

Organophosphorus pesticides (OPPs), a group of organophosphate or phosphate sulphide esters, are prevalent insecticides commonly applied worldwide in agricultural, residential, and commercial settings with the advantages of their cost-effectiveness and high efficacy in controlling pests and preventing insect-borne diseases<sup>[7]</sup>. Nevertheless, the persistent non-biodegradable nature and propensity of residues accumulation in soil and water bodies in conjunction with multiple routes of human exposure to OPPs, for instance, ingestion, inhalation, and skin contact have raised public attention to concern about their toxic effects on human health and ecosystems<sup>[8]</sup>. Part of OPPs can be swiftly absorbed, metabolized, and eliminated as urinary dialkyl phosphate (DAP) metabolites from the body, commonly used as biomarkers in cohort studies<sup>[9]</sup>. Currently, available research has found that exposure to OPPs is relevant to diverse diseases in general adults, including cancer<sup>[10]</sup>, central nervous system disorders (Parkinson's disease<sup>[11]</sup> and depression<sup>[12]</sup>), sleep problem<sup>[13]</sup>, diabetes<sup>[14]</sup>, hypertension<sup>[15]</sup>, sex hormone function<sup>[16]</sup>, and atopic diseases<sup>[17]</sup>. Limited evidence explored a potential link between exposure to pesticides and impaired retinal function. Several sporadic case series reported observations of macular disorders in patients with histories of pesticides exposure<sup>[18-21]</sup>, suggesting the harmful macular sequelae of multifarious kinds of pesticides. Only a survey built upon the Agricultural Health Study preliminarily revealed the association between macular degeneration and usage history of OPPs within specific occupational groups, but ignoring the relationships between single pattern and combined DAP metabolites and the development of AMD<sup>[22]</sup>. Thus, advanced techniques are need to be introduced to gain a deeper insight into the under-researched relationships.

Machine learning (ML) models are featured with excellent generalizability and differentiability that can provide accurate predictions and analyze complex nonlinear relationships between exposure covariates and disease prognosis by training and validating models<sup>[23]</sup>. In recent years, with the gradual and widespread application of ML models, they are increasingly proposed for automated detection, screening, classification, monitoring, and prediction of AMD primarily in the context of imaging and clinical parameters, such as

fundus autofluorescence images, color fundus photographs, optical coherence tomography, and visual acuity to improve the reliability and trustworthiness<sup>[24-26]</sup>. However, ML applied for prediction AMD by metabolites from serum<sup>[27]</sup> or urine<sup>[28]</sup> is still insufficient, as well as without utilization of interpretable ML (IML) models in identifying risk factors for AMD.

NHANES is a cross-sectional survey on U.S. population attempting to picture the nationwide health and nutritional status. We extracted urinary DAP metabolites from the two NHANES cycles between 2005 and 2008 to construct an ML model for AMD prediction, followed by application of several IML methods, including permutation feature importance (PFI) analysis, partial dependence plot (PDP) analysis, and SHapley Additive exPlanations (SHAP) analysis to the predictive model, in order to evaluate the contribution weight of each feature to the prediction outcome, to demonstrate relationships from local and global perspectives, and to investigate interactions among all variables included. As a result, the main objective of our study was to utilize ML approaches to make a description of the associations between urinary DAP metabolites and AMD risk, which could enable ML to serve as a risk indicator for AMD development.

## PARTICIPANTS AND METHODS

**Ethical Approval** The NHANES program was approved and authorized by the National Center for Health Statistics (NCHS) Research Ethics Review Board. All participants recruited had provided written informed consent. All methods and procedures were performed in accordance with the relevant guidelines and regulations.

**Data Source and Study Population** NHANES, a cross-sectional survey with a multi-stage and stratified sampling design, conducted by the NCHS and the Centers for Disease Control and Prevention (CDC), aims to understand nationwide health and nutritional status of the U.S. population and to identify disease risk factors. Participants were voluntary to provide socio-demographic information, complete standardized personal questionnaires, undergo physical examinations, and receive laboratory tests. This research was carried out by utilizing the publicly available datasets which can be accessed at the following website: <https://www.cdc.gov/nchs/nhanes/index.htm>.

In this article, we presented data from the two consecutive NHANES cycles (2005–2006 and 2007–2008), because only these two cycles included both AMD and OPPs information. Initially, we enrolled a total of 36 721 study participants, and 543 individuals were removed with missing sample weight. From these, we screened a subsample of 36 178 participants, and excluded records with missing data on AMD ( $n=30\ 574$ ). Therefore, we further removed participants lack of data on urinary DAP metabolites and other covariate information

( $n=3759$ ) to obtain consistent and accurate results. Ultimately, 1845 participants were retained for the final statistical analysis, of whom 137 had AMD. The selection process methodology is outlined in the flowchart presented in Figure 1.

**Outcome Assessment** The main outcome of this study was diagnosis of AMD dependent on fundus examination performed by the retinal camera (CR6-45NM Non-Mydriatic Retinal Camera and EOS 10D digital camera; Canon USA, Inc, Lake Success, New York) for the NHANES survey. Each image was then graded by at least two experienced ophthalmic raters according to a rigorous procedure of the Wisconsin Age-Related Maculopathy Grading System. The classification of AMD was determined on the condition of the worse eye, if data were available for both eyes, and categorized into 3 severity levels, no AMD, early AMD, or late AMD. Early AMD was defined by the presence or absence of drusen and/or pigmentary abnormalities, while late AMD by the signs of exudative AMD and/or geographic atrophy. In this research, patient with AMD was defined as the presence of early or late AMD in either eye. All 1845 participants were divided into AMD ( $n=137$ ) and no AMD ( $n=1708$ ) groups on the basis of this diagnostic criterion.

**Measurement of Urinary DAP Metabolites** The concentrations of DAPs in urine reflects the non-specific metabolites of OPPs and are commonly utilized as indicators that allow for the direct measurement of exposure to OPPs and evaluation of overall health status of individuals.

Six DAP metabolites covered almost the majority of OPPs registered in the U.S. Environmental Protection Agency, consisting of dimethylphosphate (DMP), dimethylthiophosphate (DMTP), dimethyldithiophosphate (DMDTP), diethylphosphate (DEP), diethylthiophosphate (DETP), and diethyldithiophosphate (DEDT) reported in this study. Concisely, the concentrations of DAPs were examined by ultrahigh performance liquid chromatography-tandem mass spectrometry (UHPLC-MS) based on solid phase extraction (SPE) coupled with isotope dilution pre-treatment and corrected by urinary estimated glomerular filtration rate (eGFR). To ensure consistency and reliability for public health surveillance, NHANES employed a comprehensive quality control and quality assurance program. Details on laboratory measurement methods, as well as procedures for sample collection and processing are available in the NHANES Laboratory Procedure Manual on official website.

**Demographic Covariates** Information on covariates was gathered through a combination of computer-assisted personal interview, physical examination, and laboratory assessment. Socio-demographic variables, including ethnicity (non-Hispanic white, non-Hispanic black, Mexican American, or other), marital status (married or living with partner, unmarried

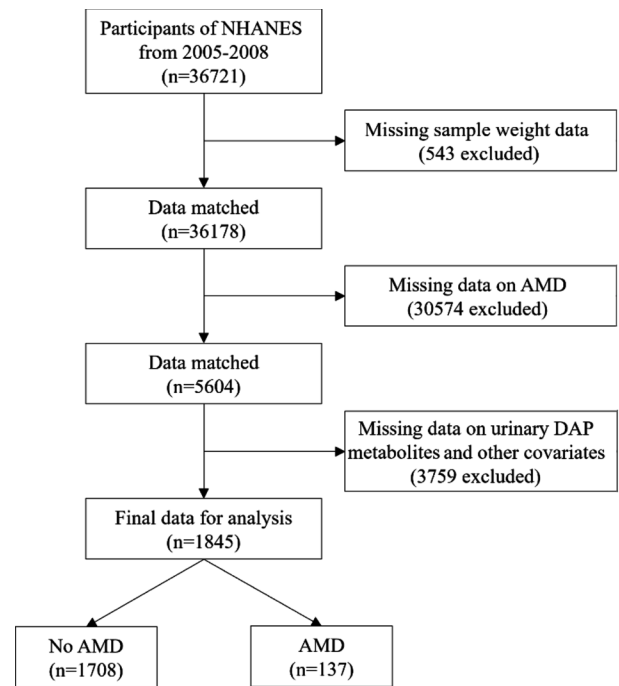


**Figure 1** Flow chart of participant selection for the final analysis NHANES: National Health and Nutrition Examination Survey; AMD: Age-related macular degeneration; DAP: Dialkyl phosphate.

or other), educational background (below high school, high school or above), poverty income ratio (PIR), smoking status (never, former, current smoking), alcohol consumption (never, former, mild, moderate, heavy drinking), body mass index (BMI), total energy intake (kcal/d), and healthy eating index (HEI) score were incorporated into our model and were classified in conformity with their respective criteria.

In light of the considerable influences that chronic diseases, including hypertension, diabetes mellitus, and chronic kidney disease (CKD) exerted on the risk of AMD, the inclusion of participants' self-reported diagnoses of these ailments into the study enhanced the comprehensiveness of AMD risk prediction model. Within the above covariates, specifically, BMI was calculated as measured weight (kg) divided by the square of height ( $m^2$ ). PIR, an index of household's total income to define the economic status, was set at a value of 1.00 to correspond with the official federal poverty threshold level. The presence of CKD was defined by a decreased eGFR of lower than  $60 \text{ mL/min}\cdot 1.73 \text{ m}^2$ , according to the Chronic Kidney Disease Epidemiology Collaboration creatinine equation.

**Construction of Machine Learning Models** The total dataset was randomly divided into two distinct subsets, in which 80% as the training set ( $n=1708$ ) and 20% as the test set ( $n=137$ ), via five-fold cross-validation resampling method to provide a more thorough assessment of the generalization ability of the model. Subsequently, eleven different ML algorithms, including Random Forest (RF), XGBoost (XGB), Gaussian

Process (GP), Naive Bayes (NB), K-Nearest Neighbour (KNN), C5.0 Decision Trees (C5.0), Neural Network (NN), Gradient Boosting Machine (GBM), Multi-Layer Perceptron (MLP), Logistic Regression (LR), and Supported Vector Machine (SVM) were constructed for AMD prediction with the training set. Each ML algorithm was trained and tuned on different permutations of the training data, and the effect was examined by the testing set.

**Evaluation of Machine Learning Models** The performance of each ML algorithm model was estimated through various evaluation metrics, including the area under the curve (AUC) of receiver operating characteristic curve (ROC), apparent prevalence, true prevalence, sensitivity, specificity, positive predictive value (PPV), negative predictive value (NPV), positive likelihood ratio (PLR) and negative likelihood ratio (NLR). These evaluation indicators were calculated based on the testing set *via* the following R packages: “caret”, “randomForest”, “pROC”, “stats”, “epiR”, “ggplot2”, “dplyr”.

**Interpretation of Prediction Model** Interpretability methods were classified into two categories: global and local. The global model-agnostic methods comprised of PFI analysis, PDP analysis, accumulated local effects (ALE) plot, and feature interaction quantification. As for the local model-agnostic methods, individual conditional expectation (ICE) plot, local interpretable model-agnostic explanations (LIME), Shapley values, and SHAP method were contained. All these approaches were integrated into the prediction model to systematically evaluate the contribution of urinary DAP metabolites and baseline characteristics to the prediction of AMD risk.

Briefly, global model-agnostic methods described the typical behavior of an ML model, proving invaluable in exploring the overarching patterns and underlying the inherent mechanisms in the data. PFI analysis determined the significance of a feature as an increase in the model’s prediction error loss after the variable was permuted, arousing a more intuitive quantification of the contribution of each DAP metabolite to the prediction of AMD risk. In parallel, SHAP importance analysis had similarities to a variance-based importance measure, contrasting with the loss-based definition as in the case of PFI<sup>[29]</sup>. PDP analysis furnished an explanation to observe the marginal effect of each individual covariate on the outcome and to average the corresponding of variables predicted by the model<sup>[30]</sup>. ALE plot focused on the accumulative effect, offering a more precise depiction when dealing with correlated features, which served as a faster and unbiased alternative to PDP<sup>[31]</sup>. Feature interaction quantification was performed when features interacted with each other in a prediction model, in order to measure the extent to which prediction was influenced by the joint effects<sup>[32]</sup>.

With regard to local model-agnostic methods, they explained individual prediction of an ML model. ICE curve was integrated into the PDP analysis to take both the dependence of the prediction on each feature and the collective effect of changes into account, providing a detailed insight into the behavior of the model<sup>[33]</sup>. LIME was an algorithm for explaining the prediction outcome by building a simpler and interpretable model in the vicinity of the prediction of the black-box model<sup>[34]</sup>. Shapley value was an attribution method that fairly distributed the difference between the prediction and the average prediction of the model to individual covariate<sup>[35]</sup>. Through connecting LIME and Shapley value, SHAP analysis aimed to provide an extensive knowledge of the contribution made by each feature in an ML model towards the prediction result<sup>[34-35]</sup>. Both LIME and SHAP analysis were novel explainable methods adopted by researchers to solve black-box problems associated with ML models. Interpretability pipelines were implemented through the following R packages: “shapviz”, “lime”, “DMwR2”, “iml”.

**Statistical Analysis** Descriptive statistics in this study for continuous variables were reported as weighed means±standard deviation (SD) by the Student’s *t*-test or the Mann-Whitney *U* test, and for categorical variables were expressed as percentage (%) of participants in each group by the Wilcoxon two-sample test or the Chi-square test.

Logarithmic transformation was applied to normalize the skewed distributions of urinary DAP metabolites. Pearson correlation analyses were then conducted to investigate the relationships among continuous urinary DAPs and calculate Pearson correlation coefficients. Moreover, multicollinearity tests on covariates were performed to ensure the model stability by employing the variance inflation factor (VIF) in this research, where all VIF values below 10 indicated the absence of multicollinearity among all variables. Logistic regression analyses were applied to assess associations among binary categorical variables and provide regression coefficient and corresponding statistical significance.

Survey-weighted generalized linear regression models were performed to evaluate the associations between each continuous DAPs and AMD risk using adjusted odds ratios (ORs) and 95% confidence intervals (CIs). Three models were constructed. Model 1 included no adjustment for covariates. Model 2 was adjusted for age and sex. Model 3 included further adjustment for ethnicity, marital status, education, poverty ratio, smoking status, alcohol consumption, BMI, Kcal.Intake, HEI.score, hypertension, and CKD in addition to the covariates adjustment of model 2.

All calculations and analyses were performed in R software (R 4.3.0) with *P* less than 0.05 considered statistically significant.

**RESULTS**

**Demographic Characteristics of Participants** Table 1 summarizes the demographics as well as other characteristics of the participants with and without AMD in this study. Of a total of 1845 included American adults, 137 were diagnosed with AMD and 1708 with no AMD. The prevalence of AMD was 6.34% (137/1845). The mean age of the total population was 56.26±0.47y, with 67.17±1.59 and 55.52±0.41y in each group, respectively. Women comprised 53.26% of the subject population, slightly more than men (46.74%), with no significant difference ( $P=0.22$ ). Aged 40-49 (35.27%), non-Hispanic White (75.57%), married or living with a partner (68.26%), with high school or above levels of education (83.18%), at or above poverty line (90.25%), never smoking (50.33%), mild alcohol drinking (39.03%), BMI ranging from 18.5 to 30.0 kg/m<sup>2</sup> (60.91%), without hypertension (51.69%) and without diabetes (71.97%) accounted for the largest proportions of the total population. Furthermore, there were substantial variations between AMD and no AMD groups in terms of age, ethnics, marital status, smoking status, hypertension and CKD ( $P<0.05$ ).

**Statistical Analysis and Variables Selection** Pearson correlation results indicated that most of the DAP metabolites were correlated with each other in varying degrees, with moderately strong correlations between DMTP and DMDTP ( $r=0.62$ ), DMP and DMTP ( $r=0.58$ ), DETP and DEDT ( $r=0.56$ ), DMP and DMDTP ( $r=0.54$ ) and between DMDTP and DEDT ( $r=0.52$ ) among 1845 subjects (Figure 2). Moreover, multicollinearity analysis using VIFs implied that there was no multicollinearity between the DAPs and covariates.

**Associations Between DAP Metabolites and AMD Risk** Survey-weighted generalized linear regression model results showed no significant correlations between any of six DAPs and AMD risk in both the crude model and models adjusted for related demographic or other covariates (Table 2). Because traditional generalized linear models have limitations (*e.g.*, restrictive distributional assumptions and low sensitivity to weak effects), we attempted to adopt ML approaches to better characterize potential subtle yet complex associations.

**Evaluation and Comparison of Eleven Machine Learning Models Predictive Capabilities** As depicted in Figure 3, ROC analysis curves of all selected ML models demonstrate the efficacy of identification of AMD risk from the testing set. The AUC value of the RF model was observed to be 0.688, XGBoost (0.665), GP (0.659), NB (0.652), KNN (0.642), C5.0 (0.633), NN (0.629), GBM (0.625), MLP (0.617), LR (0.615), and SVM (0.602), based on the testing set. Eleven inclusive models achieved comparable predictive performances detailed in the discriminative features, including apparent prevalence, true prevalence, sensitivity, specificity, PPV, NPV, PLR and



**Figure 2 Pearson correlations of urinary DAP metabolites factors among 1845 subjects** Pearson correlations between six continuous DAP metabolites. DAP: Dialkyl phosphate; DMP: Dimethylphosphate; DEP: Diethylphosphate; DMTP: Dimethylthiophosphate; DETP: Diethylthiophosphate; DMDTP: Dimethyldithiophosphate; DEDT: Diethyldithiophosphate.

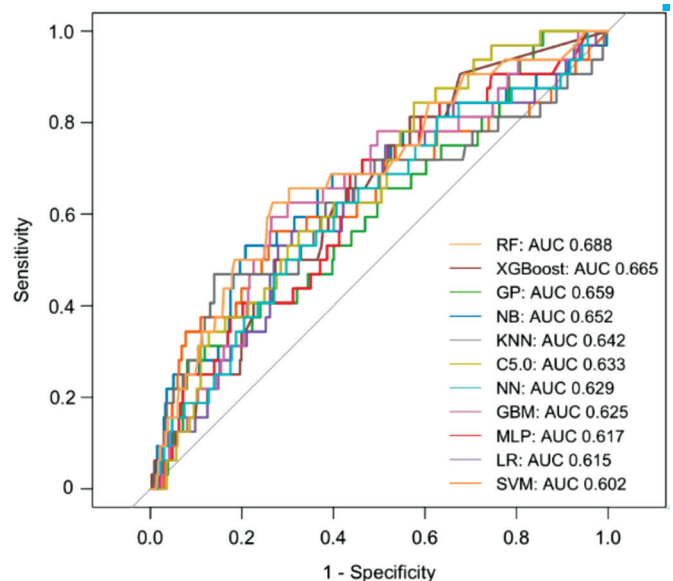


**Figure 3 ROC analysis curves of eleven ML models based on the testing set** ML model was utilized to fit the prediction between AMD risk and urinary DAP metabolites. ROC: Receiver operating characteristic curve; ML: Machine learning; AMD: Age-related macular degeneration; DAP: Dialkyl phosphate; AUC: Area under the curve; RF: Random Forest; GP: Gaussian Process; NB: Naive Bayes; KNN: K-Nearest Neighbour; C5.0: C5.0 Decision Trees; NN: Neural Network; GBM: Gradient Boosting Machine; MLP: Multi-Layer Perceptron; LR: Logistic Regression; SVM: Supported Vector Machine.

NLR (Table 3). Accordingly, these findings highlighted that the predictive ability of the RF model was superior among these learning models, hence, the RF-based prediction model was finally selected for subsequent assessment.

**Table 1 Baseline characteristics of participants**

*n* (%) or mean±SD

Variables	Total, <i>n</i> =1845	No AMD, <i>n</i> =1708 (93.66)	AMD, <i>n</i> =137 (6.34)	<i>P</i>
Age (y)	56.26±0.47	55.52±0.41	67.17±1.59	<0.0001
40-49	494 (35.27)	483 (36.60)	11 (15.56)	
50-59	449 (29.56)	436 (30.69)	13 (12.91)	
60-69	444 (17.72)	417 (17.69)	27 (18.24)	
≥70	458 (17.45)	372 (15.02)	86 (53.29)	
Sex				0.22
Male	923 (46.74)	846 (46.38)	77 (51.99)	
Female	922 (53.26)	862 (53.62)	60 (48.01)	
Ethnicity				0.002
Non-Hispanic White	974 (75.57)	874 (74.72)	100 (88.10)	
Non-Hispanic Black	371 (9.47)	360 (9.86)	11 (3.61)	
Mexican American	299 (5.67)	284 (5.79)	15 (3.89)	
Other	201 (9.30)	190 (9.63)	11 (4.41)	
Marital status				0.01
Unmarried or other	677 (31.74)	618 (31.10)	59 (41.30)	
Married or living with a partner	1168 (68.26)	1090 (68.90)	78 (58.70)	
Educational background				0.75
Below high school	534 (16.82)	499 (16.75)	35 (17.81)	
High school or above	1311 (83.18)	1209 (83.25)	102 (82.19)	
Poverty ratio				0.54
Below poverty line (<1.00)	302 (9.75)	277 (9.67)	25 (10.83)	
At or above poverty line (≥1.00)	1543 (90.25)	1431 (90.33)	112 (89.17)	
Smoke				0.001
Never	876 (50.33)	815 (50.94)	61 (41.45)	
Former	588 (29.34)	530 (28.16)	58 (46.69)	
Current	381 (20.33)	363 (20.90)	18 (11.87)	
Alcohol use				0.37
Never	258 (11.88)	234 (11.58)	24 (16.21)	
Former	479 (22.60)	438 (22.27)	41 (27.45)	
Mild	638 (39.03)	590 (39.24)	48 (35.93)	
Moderate	242 (14.37)	230 (14.75)	12 (8.77)	
Heavy	228 (12.13)	216 (12.16)	12 (11.64)	
BMI (kg/m <sup>2</sup> )	29.03±0.18	29.08±0.19	28.26±0.52	0.16
BMI				0.07
18.5-30.0	1106 (60.91)	1006 (59.99)	100 (74.53)	
<18.5	27 (1.40)	27 (1.50)	0 (0.00)	
≥30.0	712 (37.69)	675 (38.51)	37 (25.47)	
Kcal.Intake (kcal/d)	2091.29±28.05	2097.56±28.00	1998.55±109.92	0.38
HEI.score	51.06±0.42	51.04±0.45	51.30±1.63	0.89
Hypertension				0.02
No	840 (51.69)	794 (52.51)	46 (39.48)	
Yes	1005 (48.31)	914 (47.49)	91 (60.52)	
Diabetes				0.44
No	1224 (71.97)	1136 (72.22)	88 (68.28)	
Yes	621 (28.03)	572 (27.78)	49 (31.72)	
CKD	85.76±0.74	86.52±0.67	74.53±2.50	<0.0001
Exposures (μg/L)				
DMP	-4.28±0.06	-4.29±0.06	-4.13±0.18	0.41
DEP	-4.87±0.05	-4.89±0.06	-4.66±0.15	0.17
DMTP	-3.79±0.06	-3.80±0.06	-3.72±0.15	0.62
DETP	-5.01±0.03	-5.01±0.03	-5.05±0.08	0.57
DMDTP	-5.08±0.04	-5.08±0.04	-5.11±0.10	0.72
DEDT	-5.75±0.03	-5.75±0.03	-5.78±0.07	0.71

BMI: Body mass index; Kcal: Kilocalorie; HEI: Healthy eating index; CKD: Chronic kidney disease; DMP: Dimethylphosphate; DEP: Diethylphosphate; DMTP: Dimethylthiophosphate; DETP: Diethylthiophosphate; DMDTP: Dimethyldithiophosphate; DEDT: Diethyldithiophosphate.

**Table 2 Comparison between different models of the weighted relationship between organophosphorus pesticides and risk of AMD**

Exposures (µg/L)	Model 1		Model 2		Model 3	
	OR (95%CI)	P	OR (95%CI)	P	OR (95%CI)	P
DMP	1.03 (0.91, 1.16)	0.63	1.04 (0.91, 1.18)	0.60	1.02 (0.90, 1.16)	0.74
DEP	1.04 (0.92, 1.18)	0.50	1.03 (0.90, 1.18)	0.69	1.02 (0.89, 1.16)	0.75
DMTP	1.06 (0.90, 1.25)	0.48	0.96 (0.80, 1.15)	0.65	0.96 (0.80, 1.15)	0.65
DETP	0.86 (0.65, 1.11)	0.26	0.83 (0.62, 1.09)	0.20	0.85 (0.64, 1.11)	0.25
DMDTP	1.06 (0.86, 1.31)	0.58	1.08 (0.85, 1.35)	0.53	1.07 (0.85, 1.34)	0.53
DEDT	1.04 (0.77, 1.37)	0.80	1.02 (0.74, 1.38)	0.88	0.97 (0.70, 1.32)	0.86

Model 1: Not adjusted for any covariates; Model 2: Adjusted for age and sex; Model 3: Adjusted for ethnicity, marital status, education, poverty ratio, smoking status, alcohol consumption, BMI, Kcal.Intake, HEI.score, hypertension, and CKD in addition to adjustments given for model 2; DMP: Dimethylphosphate; DEP: Diethylphosphate; DMTP: Dimethylthiophosphate; DETP: Diethylthiophosphate; DMDTP: Dimethylidithiophosphate; DEDT: Diethylidithiophosphate; OR: Odds ratio; CI: Confidence interval.

**Interpretable Pipelines**

**Predictor variable importance** Technique such as PFI analysis provided a comprehensive understanding of the contribution weight of each variable in the prediction model. LIME algorithm (Figure 4A) was employed to rank the significance of DAP metabolites (DMP, DEP, DMTP, DETP, DMDTP and DEDT) and individual baseline characteristics (age, sex, BMI, ethnicity, alcohol using, smoking status, education level, marital status, poverty ratio, etc.) in the RF model, in which their descending sequence indicated their magnitude of effect. According to the LIME method, the principal influencing factors lied on age, followed by DEDT, CKD, DMTP, DETP, DEP, DMP and BMI, suggesting that all six urinary DAP metabolites contributed considerable weights in predicting the risk of AMD.

Figure 4B-4D display the variables contributing to the predictive value of AMD risk as assessed by SHAP method. The SHAP feature importance bar chart (Figure 4B) exhibits the general effects of DAP metabolites and baseline variables on the risk of AMD. The absolute SHAP value was taken into account when ranking the features, regardless of the positive or negative effect to the model output. Covariates with higher mean absolute SHAP values were determined as being more influential to the prediction of AMD, ranked from top to bottom in accordance with the importance.

Furthermore, the SHAP summary plot (Figure 4C) validates a more detailed information of the DAPs compared with the bar chart. As depicted by Figure 4D, SHAP analysis identifies the contributions of six DAP metabolites in influencing the AMD risk, which categorizes DMTP as the most critical parameter, higher than any other metabolites.

The SHAP algorithm showed a similar pattern as the LIME algorithm for the status of DAP metabolites among all covariates. Concretely speaking, DAP metabolites ranked first among all variances, moreover, age, CKD, BMI and HEI score had certain impact on the prediction of AMD risk. It was

worth noting that the contribution weights of demographic characteristics and lifestyle-related variables in the prediction of AMD risk in our results were lower compared to OPPs exposure, and all baseline characteristics variables except age and CKD status were weaker than DAP metabolites under two different investigation algorithms.

**Predictive modeling visualization** The individual decision-making process for the prediction of AMD risk was evaluated by Shapley value and visualized by SHAP waterfall plot to interpretate the degree of each feature contributing to the overall outcome.

Defined as the average marginal contribution of a feature value across all possible coalitions, the Shapley value was employed to examine the prediction of AMD risk by RF model. We selected the first, 10<sup>th</sup>, 100<sup>th</sup>, and 1000<sup>th</sup> participants respectively to test the ability of model in disease prediction. For example, Figure 5A presents the Shapley values for the first individual in the AMD prediction dataset. With a prediction of -0.00, the AMD probability of this specific person was 0.08 below the average prediction of 0.08. The DMTP level exerted the most substantial negative impact, whereas the DEDT level showed a positive contribution notably distinct from the other covariates. The sum of Shapley values yielded the difference between actual and average prediction (-0.08).

In the waterfall plot, each horizontal level described how the positive (yellow) or negative (red) contribution of each feature shifted the anticipated model output  $Ef(x)$  toward the ultimate model prediction  $f(x)$ , taking into account the evidence from all the features present. For instance, Figure 6A portrays an individual aged 64 with eGFR value of 61.3 whose virtually all metabolites (DEDT, DMTP, DMDTP, DEP and DETP) contributed negatively to AMD prediction, leading to an output of 1.07.

The SHAP person waterfall plots for a range of subjects revealed a clear depiction of susceptibility to DAP metabolites, thereby highlighting the predictive capacity of ML as a

Table 3 Details on the predictive performance of eleven ML models performed in the testing set

Characteristics	SVM	NN	MLP	GP	GBM	LR	NB	XGB	C5.0	KNN	RF
Apparent prevalence	1.00 (0.99, 1.00)	1.00 (0.99, 1.00)	1.00 (0.99, 1.00)	1.00 (0.99, 1.00)	0.99 (0.98, 1.00)	1.00 (0.99, 1.00)	0.95 (0.92, 0.97)	0.99 (0.98, 1.00)	1.00 (0.98, 1.00)	1.00 (0.99, 1.00)	1.00 (0.99, 1.00)
True prevalence	0.91 (0.88, 0.94)	0.91 (0.88, 0.94)	0.91 (0.88, 0.94)	0.91 (0.88, 0.94)	0.91 (0.88, 0.94)	0.91 (0.88, 0.94)	0.91 (0.88, 0.94)	0.91 (0.88, 0.94)	0.91 (0.88, 0.94)	0.91 (0.88, 0.94)	0.91 (0.88, 0.94)
Sensitivity	1.00 (0.99, 1.00)	1.00 (0.99, 1.00)	1.00 (0.99, 1.00)	1.00 (0.99, 1.00)	0.99 (0.98, 1.00)	1.00 (0.99, 1.00)	0.95 (0.92, 0.97)	0.99 (0.98, 1.00)	1.00 (0.98, 1.00)	1.00 (0.99, 1.00)	1.00 (0.99, 1.00)
Specificity	0.00 (0.00, 0.11)	0.00 (0.00, 0.11)	0.00 (0.00, 0.11)	0.00 (0.00, 0.11)	0.00 (0.00, 0.11)	0.00 (0.00, 0.11)	0.09 (0.02, 0.25)	0.00 (0.00, 0.11)	0.00 (0.00, 0.11)	0.00 (0.00, 0.11)	0.00 (0.00, 0.11)
PPV	0.91 (0.88, 0.94)	0.91 (0.88, 0.94)	0.91 (0.88, 0.94)	0.91 (0.88, 0.94)	0.91 (0.88, 0.94)	0.91 (0.88, 0.94)	0.92 (0.88, 0.94)	0.91 (0.88, 0.94)	0.91 (0.88, 0.94)	0.91 (0.88, 0.94)	0.91 (0.88, 0.94)
NPV	NaN (0.00, 1.00)	NaN (0.00, 1.00)	NaN (0.00, 1.00)	NaN (0.00, 1.00)	0.00 (0.00, 0.84)	NaN (0.00, 1.00)	0.15 (0.03, 0.38)	0.00 (0.00, 0.84)	0.00 (0.00, 0.97)	NaN (0.00, 1.00)	NaN (0.00, 1.00)
PLR	1.00 (1.00, 1.00)	1.00 (1.00, 1.00)	1.00 (1.00, 1.00)	1.00 (1.00, 1.00)	0.99 (0.99, 1.00)	1.00 (1.00, 1.00)	1.05 (0.93, 1.17)	0.99 (0.99, 1.00)	1.00 (0.99, 1.00)	1.00 (1.00, 1.00)	1.00 (1.00, 1.00)
NLR	NaN (NaN, NaN)	NaN (NaN, NaN)	NaN (NaN, NaN)	NaN (NaN, NaN)	Inf (NaN, Inf)	NaN (NaN, NaN)	0.54 (0.17, 1.74)	Inf (NaN, Inf)	Inf (NaN, Inf)	NaN (NaN, NaN)	NaN (NaN, NaN)

SVM: Supported vector machine; NN: Neural network; MLP: Multi-layer perceptron; GP: Gaussian process; GBM: Gradient boosting machine; LR: Logistic regression; NB: Naive Bayes; XGB: XGBoost; C5.0: C5.0 Decision Trees; KNN: K-Nearest Neighbour; RF: Random forest; PPV: Positive predictive value; NPV: Negative predictive value; PLR: Positive likelihood ratio; NLR: Negative likelihood ratio.

sensitive model algorithm in identifying different patients for disease risk forecasting. Within the subset of four randomly selected patients, DAP metabolites occupied prominent positions in the variety of influencing factors, thereby accentuating the indispensable role of DAP metabolites in predicting AMD risk. The results pointed to the likelihood that continuous monitoring and assessing the urinary metabolites levels for the purposes of early detection, warning, and intervention will enhance public health security and individual well-being.

**Relationships between DAP metabolites and AMD** PDP combined with ICE (Figure 7) is implemented for an intuitive explanation on the relationship between a set of urinary DAP metabolites (DMP, DEP, DMTP, DETP, DMDTP and DEDT) and the average AMD prediction value in the RF model. The collective trajectory of the six DAP metabolites appeared as a relatively flat line from an overall perspective, implying a less pronounced impact of these features on the model's predictive outcomes for AMD. This observation may indicate that the range of DAP metabolites concentrations within the dataset did not vary significantly, or that the model did not ascribe a substantial predictive weight to these metabolites relative to the other characteristics. Considering another aspect, features with shallow PDP were assigned a lower priority in terms of immediate impacts on the AMD risk, but exerted a profound influence on the outcomes of a study in an accumulation or an interaction sense which were obscured in PDP-based analysis. Therefore, ALE plots (Figure 8) were subsequently introduced to estimate the difference of local predictions for small changes around each level of exposure, as an alternative to PDP analysis, providing a more accurate representation. We can infer several associations from the graphical representations presented. Despite essentially unchanged when DEP and DEDT were at low doses, the predicted risk of AMD escalated quickly when the ln-transformed levels of DEP and DEDT were elevated at relatively high concentration as a clear positive slope, indicating that there was a significant dose-dependent relationship between the variable and outcome. This evidence led us to speculate that higher values of DEP and DEDT had an increasingly positive effect on the average predicted AMD. In comparison, the graphs displayed similar U-shaped patterns across the remaining features investigated (DMP, DMTP, DMDTP and DETP), suggesting that these variables did not have a crucial impact on the incidence of AMD. In summary, although the PDP analysis indicated that the overall impact of DAP metabolites on the predictive risk for AMD was relatively weak, given the accumulative effects of most environmental exposures, the ALE plots further elucidated the association between exposures and outcome, indicating that certain metabolites contributed notably to the

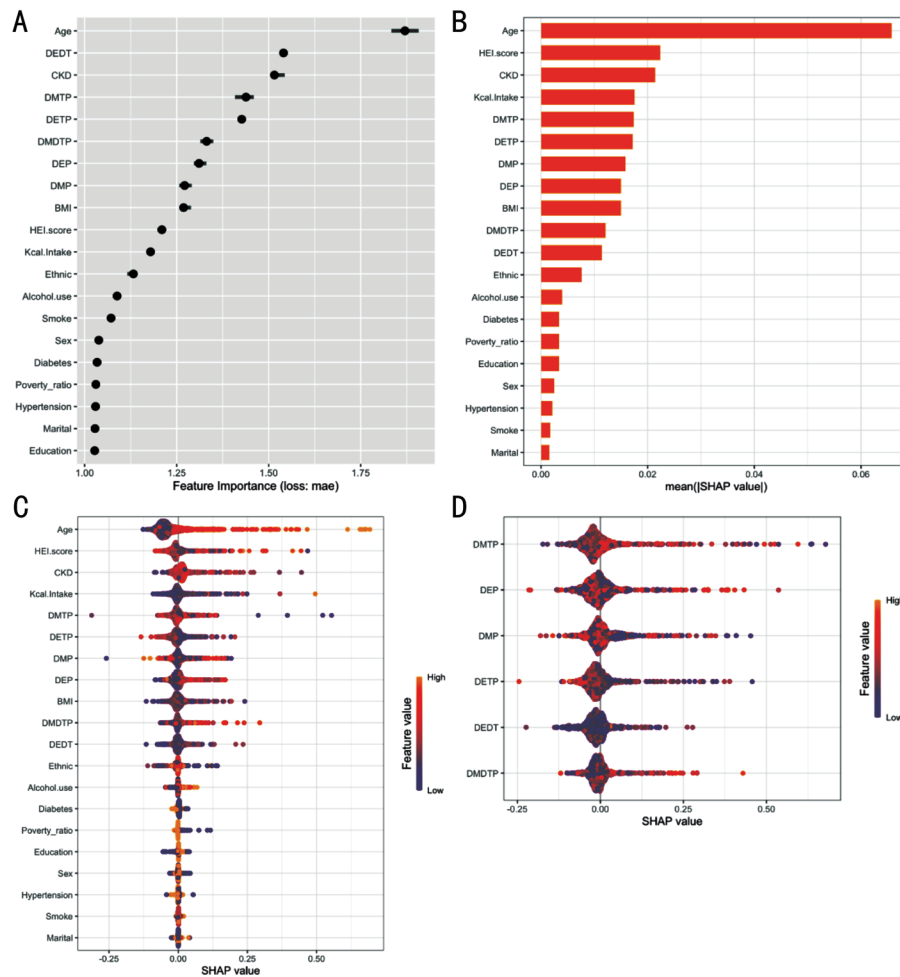


**Figure 4** Feature importance analysis for RF model in predicting the risk of AMD A: LIME feature importance forest map. The map displayed the contribution weight of each variable comprising DAP metabolites and individual baseline characteristics to the prediction of AMD using the feature importance analysis for RF model; B: SHAP feature importance bar chart. The impact of each feature on the model output was weighed by the mean absolute SHAP value for the entire dataset, in which their decreasing order indicated their utmost importance; C: SHAP feature importance summary plot; D: SHAP summary plot of six DAP metabolites and AMD risk. Each dot corresponded to the SHAP value for an individual, extending linearly along the x-axis. The orientation on the x-axis indicated the probability of developing AMD, with the movement towards the right suggesting an increased risk and towards the left indicating a reduced risk. A higher SHAP value on the x-axis represented a stronger contribution to the prediction of AMD risk. The color of each dot manifested the prediction feature value of each individual, encoded in a gradient from the yellow (high) to purple (low). The distribution of SHAP values for each feature can be visually illustrated by the y-axis deviation of the overlapping points. RF: Random Forest; AMD: Age-related macular degeneration; DEDT: Diethyldithiophosphate; CKD: Chronic kidney disease; DMTP: Dimethylthiophosphate; DETP: Diethylthiophosphate; DMDTP: Dimethylidithiophosphate; DEP: Diethylphosphate; DMP: Dimethylphosphate; BMI: Body mass index; HEI: Healthy eating index; Kcal: Kilocalorie; SHAP: SHapley Additive exPlanations.

prediction of AMD risk. Consequently, the influence of DAP metabolites on the predictive risk for AMD ought not to be underestimated.

**Interaction effects of DAP metabolites on AMD** As the urine metabolic products of the organism, DAP metabolites interact with each other, thus the prediction outcome cannot only be expressed as the sum of the feature effects. Additionally, we performed the exploration of interaction properties between the corresponding variables in a RF trained model to predict AMD, given some risk factors (Figure 9A). Features were observed to be prioritized in accordance with their respective overall interaction strengths, where age, BMI, DEDT, CKD, DMTP,

DEP, DETP, DMDTP, and DMP exceeded the threshold of 0.2. Notably, DEDT exhibited the most pronounced interaction effect among six DAP metabolites.

Upon evaluating the interactions among all the variables, we selected DEDT distinguished by the most considerable interaction effect (Figure 9B). Consequently, we proceeded with a detailed investigation into the two-way interactions of DEDT alongside other covariates. Several relationships can be derived from the graphs that DETP and DEDT presented the highest magnitude above 0.6, whereas the other DAPs generated critical influence on the prediction of AMD risk by DEDT, with all values surpassing 0.2.

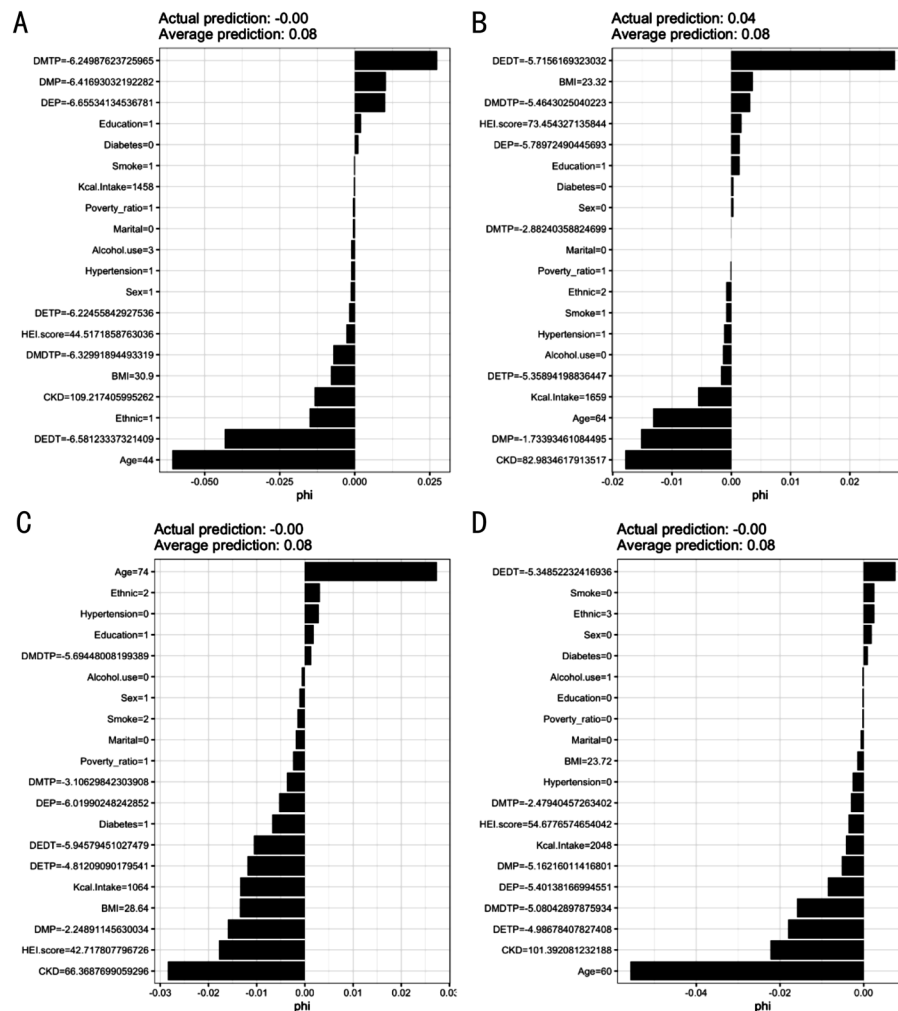


**Figure 5** Shapley value-based interpretation for individual observations of participants, to demonstrate patient profiles for predicting outcomes A: First; B: 10<sup>th</sup>; C: 100<sup>th</sup>; D: 1000<sup>th</sup>. DMTP: Dimethylthiophosphate; DMP: Dimethylphosphate; DEP: Diethylphosphate; Kcal: Kilocalorie; DETP: Diethylthiophosphate; HEI: Healthy eating index; DMDTP: Dimethyldithiophosphate; BMI: Body mass index; CKD: Chronic kidney disease; DEDT: Diethyldithiophosphate.

Apart from the global model method already discussed, we also utilized local model method to further substantiate the interacting relationships among the metabolites in the course of AMD prediction. The SHAP dependence plots (Figure 10) were applied to reveal how the Shapley values for the levels of DAP metabolites affected the model output. Corresponding with the previous results from PDP analysis, roughly speaking, the consequences hinted that the model did not solely dependent on the abundance of DAP metabolites with respect to the data distribution. In case of interactions, the SHAP dependence plots were automatically colored with the strongest interaction feature. In addition to the interactions observed among DAP metabolites, age emerged as the most potent element of interaction influencing the majority of DAPs and another critical factor was identified as CKD. Taking all these factors into account, the interaction performances of the baseline variables for predicting AMD risk remained inferior to that of urinary DAP metabolites, in conformity with the findings from several analytical

approaches, which emphasized the indispensable role of DAP metabolites in the course of AMD risk prediction. The results pointed that detection of DAP metabolites levels may be potentially vital for managing the progression of AMD.

### DISCUSSION

Our research is the first large-scale cross-sectional population-based epidemiology investigation to demonstrate the relationships between OPPs exposure and AMD risk among U.S. population. We utilized eleven ML algorithms to screen the urinary DAP metabolites data available between 2005 and 2008 from the two NHANES cycles, with the help of evaluation indicators, finally selected the best-performing RF model capable of predicting the risk of AMD. Furthermore, a series of effective parameters including PFI analysis, PDP analysis, and SHAP analysis were applied to gain a better understanding of the relationships and interactions between DAP metabolites and AMD. Our results suggested indispensable contributions from six DAP metabolites to AMD risk prediction, highlighting the capability of ML as a sensitive

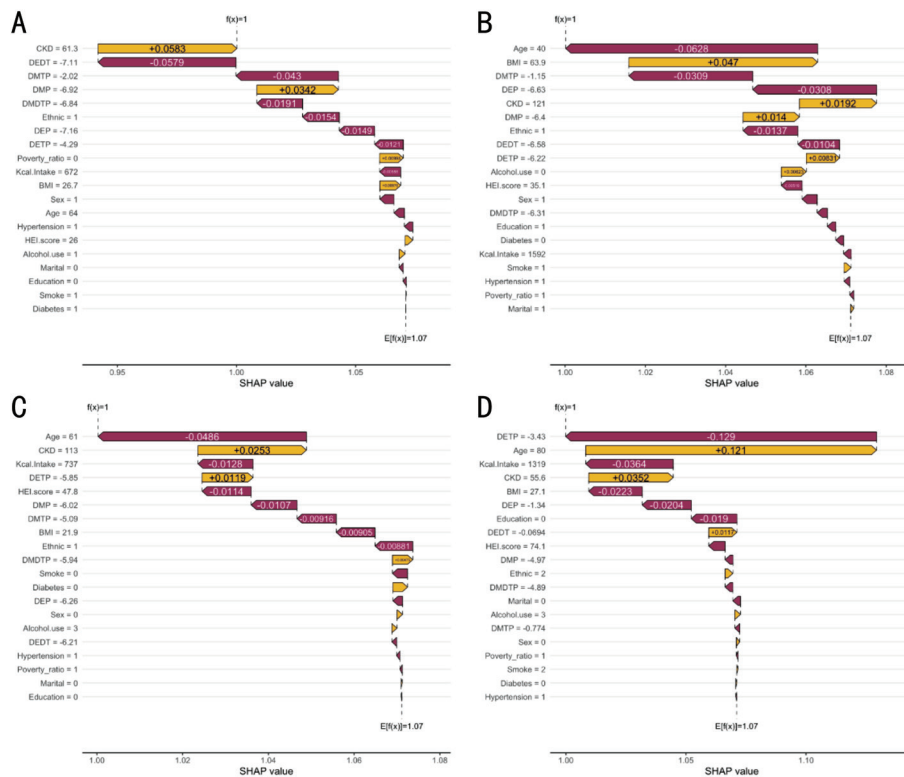


**Figure 6** The SHAP person waterfall plots of participants, to demonstrate patient profiles for predicting outcomes A: 1<sup>st</sup>; B: 10<sup>th</sup>; C: 100<sup>th</sup>; D: 1000<sup>th</sup>. SHAP: SHapley Additive exPlanations; CKD: Chronic kidney disease; DEDT: Diethylthiophosphate; DMTP: Dimethylthiophosphate; DMP: Dimethylphosphate; DMDTP: Dimethylthiophosphate; DEP: Diethylphosphate; DETP: Diethylthiophosphate; Kcal: Kilocalorie; BMI: Body mass index; HEI: Healthy eating index.

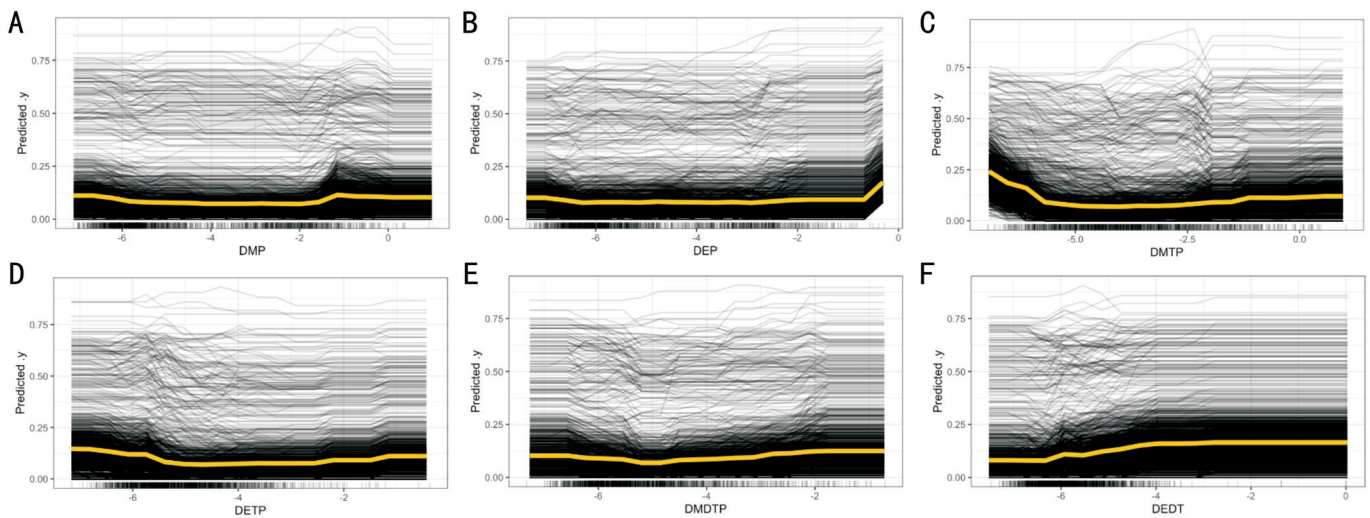


**Figure 7** PDP analysis for the relationship between ln-transformed concentrations of DAP metabolites and the average predictive AMD risk A: DMP; B: DEP; C: DMTP; D: DETP; E: DMDTP; F: DEDT. PDP: Partial dependence plot; DAP: Dialkyl phosphate; AMD: Age-related macular degeneration; DMP: Dimethylphosphate; DEP: Diethylphosphate; DMTP: Dimethylthiophosphate; DETP: Diethylthiophosphate; DMDTP: Dimethylthiophosphate; DEDT: Diethylthiophosphate.

and reliable model algorithm in predicting the risk of diseases. We screened the RF model as the outstanding learning model with its superior ability of predicting AMD based on urinary DAP metabolites exposure data through ROC analysis and corresponding AUC values. RF is a classical ML algorithm that has been frequently utilized in the course of diagnosis, monitoring and prediction of AMD, while exhibiting

the superiority of high accuracy, robustness to noise and scalability. When it comes to application ML to analyzing OPPs exposure data, only a single survey has been reported so far with the utilization of three ML approaches, namely, random forest regression, GBM and NN analysis. As a consequence, all the model performances were poor according to the ten-fold cross-validation, indicating that the information

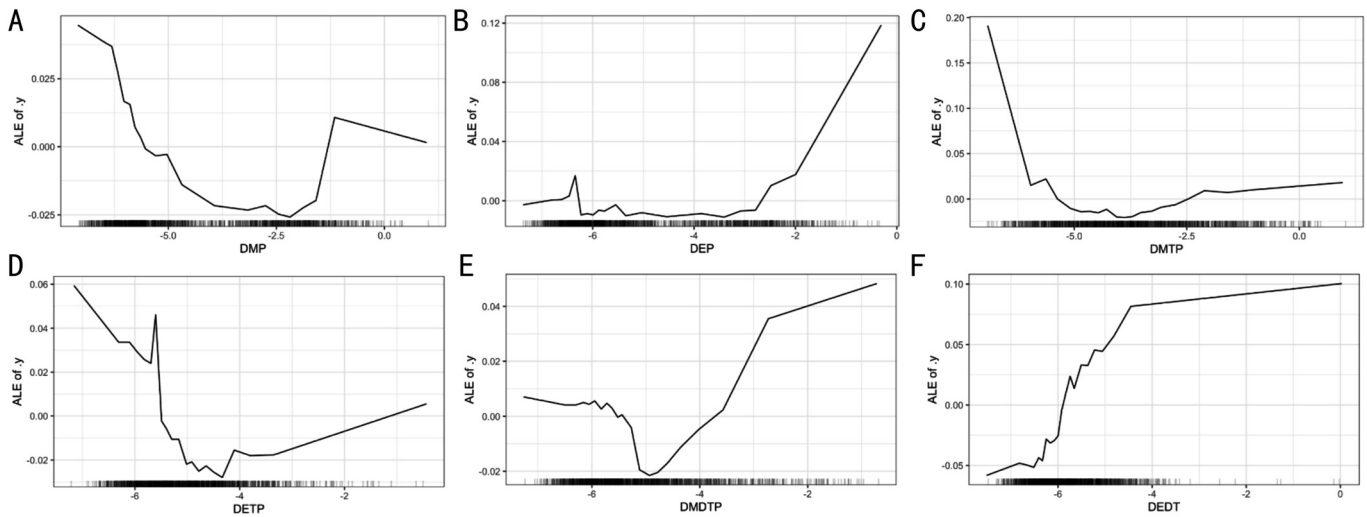


**Figure 8** ALE plots of the accumulated effects on AMD predictions for DAP metabolites A: DMP; B: DEP; C: DMTP; D: DETP; E: DMDTP; F: DEDT. ALE: Accumulated Local Effects; AMD: Age-related macular degeneration; DAP: Dialkyl phosphate; DMP: Dimethylphosphate; DEP: Diethylphosphate; DMTP: Dimethylthiophosphate; DETP: Diethylthiophosphate; DMDTP: Dimethyldithiophosphate; DEDT: Diethyldithiophosphate.

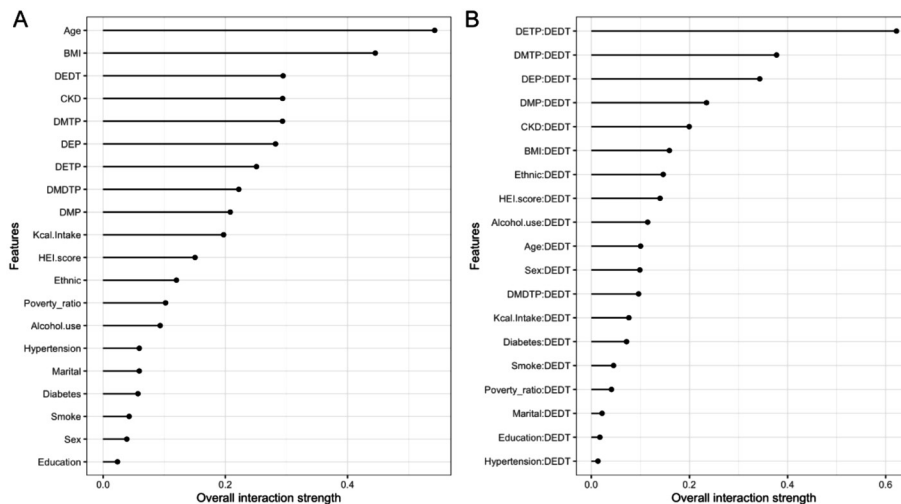


**Figure 9** The interaction effects between features on AMD risk prediction A: The interaction effects for each feature with the others on AMD risk prediction; B: The interaction effects between DEDT and the other features on AMD risk prediction. AMD: Age-related macular degeneration; BMI: Body mass index; DEDT: Diethyldithiophosphate; CKD: Chronic kidney disease; DMTP: Dimethylthiophosphate; DEP: Diethylphosphate; DETP: Diethylthiophosphate; DMDTP: Dimethyldithiophosphate; DMP: Dimethylphosphate; Kcal: Kilocalorie; HEI: Healthy eating index.

collected was insufficient to investigate predictors of urinary DAP concentrations<sup>[36]</sup>.

The combination of ML models and various interpretable methods may open the black-box of ML in the field of environmental sciences, particularly well-suited to complex and nonlinear relationships in chemical mixture exposures (e.g., multiple heavy metals<sup>[28]</sup>, air pollutants<sup>[29]</sup>, and DAP metabolites<sup>[36]</sup>). To provide a comprehensive understanding of the results generated by ML algorithms, we introduced global and local model-agnostic methods to the prediction model. Through evaluating the predictive value of each variable, PFI analysis revealed that all six urinary DAP metabolites

contributed considerable weights in the prediction of AMD risk, ranking ahead of most of the demographic characteristics and lifestyle-related variables. In an attempt to demonstrate the broad-spectrum applicability of this model, we conducted SHAP waterfall plots of randomly selected AMD individuals, underlining the predictive ability of ML as an algorithm with high accuracy and sensitivity in each case. In addition, graphical plots (PDP, ICE, and ALE) enabled visualization and accurate reflection of outcomes from RF. Methodological analyses on the properties of interactions evidently revealed the relationships and interactions between DAP metabolites and AMD risk supported by analytical statistical measures.

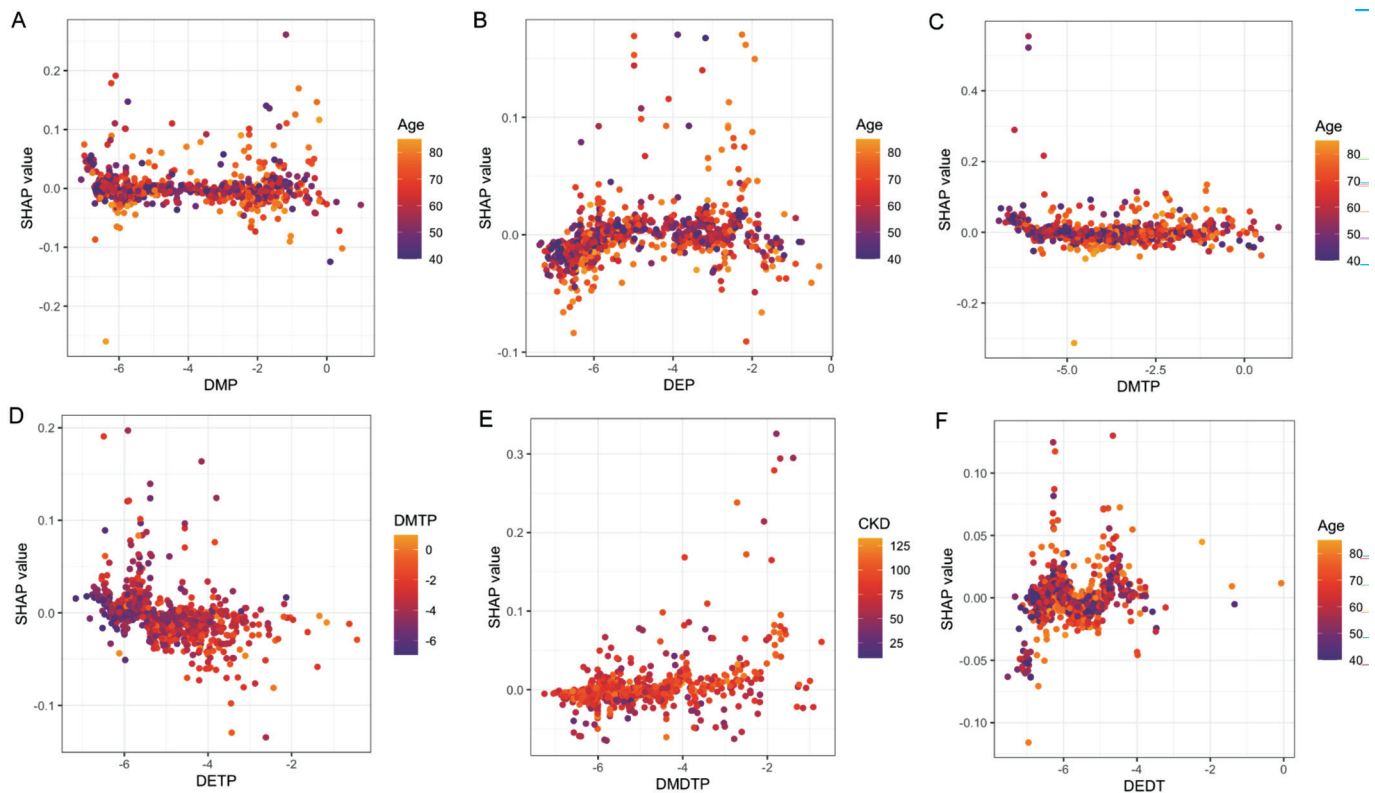


**Figure 10 SHAP dependence plots with visualized interaction to illustrate the strongest interaction factor for the level of DAP metabolites** A: DMP; B: DEP; C: DMTP; D: DETP; E: DMDTP; F: DEDT. SHAP: SHapley Additive exPlanations; DAP: Dialkyl phosphate; DMP: Dimethylphosphate; DEP: Diethylphosphate; DMTP: Dimethylthiophosphate; DEDT: Diethyldithiophosphate; DMDTP: Dimethyldithiophosphate; DETP: Diethylthiophosphate.

AMD is a chronic retinal disease involving complicated etiologic factors and has aroused public health concern and put tremendous burden on socio-economic costs worldwide<sup>[37]</sup>. However, the precise mechanisms underlying the associations between OPPs exposure and AMD remain unclear.

Of note, genetic susceptibility is a pivotal mechanism involved in the AMD pathogenesis. It has been claimed that AMD is of relevance to polymorphisms in genes participating in complement pathways, inflammation and immune regulation, lipid metabolism and transport, maintenance of the extracellular matrix, and angiogenesis<sup>[38]</sup>. At the same time, certain populations are more vulnerable to the toxic effects of environmental exposure to OPPs due to the influence of genetic polymorphisms<sup>[39]</sup>. The susceptibility to exposure can be evaluated by the common polymorphisms of cytochrome P450, glutathione transferases, acetyltransferases and paraoxonases, which are implicated in the metabolism of OPPs<sup>[40-42]</sup>. Paraoxonase 1 (PON1) has been the most studied gene for discovering its role in the development of organophosphorus-induced disorders. PON1, located on chromosome 7, is a gene encoding a protein with arylesterase and paraoxonase activity to protect against xenobiotic toxicity. Low PON1 activity increased the predisposition of the population to the OPPs poisoning<sup>[43]</sup>. Genetic polymorphisms

in PON1 affected the efficacy of the response to DNA damage in individuals exposed to OPPs<sup>[42,44]</sup>. On the other hand, PON1 genotypes have been explored in association with AMD disorders. Single nucleotide polymorphisms in the coding region of PON1, Q192R and L55M variants have been identified in the AMD patients and determined their relation to paraoxonase activity<sup>[45]</sup>. Paraoxonase activities in serum were significantly decreased in AMD patients<sup>[46]</sup>. Current studies have revealed that PON1 can be a potential risk factor for AMD but the mechanism driving AMD development has not yet been clarified. Thus, future research should concentrate on the toxicological effects in individuals susceptible to OPPs.

Oxidative stress is thought to be one of the primary drivers of the AMD development<sup>[47]</sup>. The oxidant-antioxidant imbalance is strongly implicated in the pathophysiology of AMD. Superoxide dismutase, the key enzyme required for the removal of the superoxide radical, has been reported to be significantly elevated in patients with early and late stage of AMD<sup>[48]</sup>. High levels of oxidative stress biomarkers are commonly observed in AMD patients<sup>[49]</sup> and can be further increased by aging or environmental factors, while dietary antioxidants may reduce them<sup>[50]</sup>. Exposure to chronic OPPs can produce reactive oxygen species in the retina<sup>[51]</sup> and impair the antioxidant defense system of cells<sup>[52]</sup>. Noting that

a survey conducted on the adult retinal pigment epithelial-19 cells simulating AMD *in vitro* preliminarily revealed the fact that chlorpyrifos (CPF), one of the most broadly used and hazardous OPPs, caused macular degeneration by triggering oxidative overload and established the cell model for understanding the effects of CPF exposure to ocular system<sup>[53]</sup>. Animal studies also showed that exposure to CPF brought oxidative pressure on organ tissues throughout the body<sup>[54]</sup> including ocular system<sup>[55]</sup> and interfered with the recovery of visual sensitivity in rats *in vivo*<sup>[56]</sup>. Besides, oxidative related pathway has been reported to mediate some other toxic reactions, such as genetic and epigenetic damages attributed to pesticides and organophosphorus compounds<sup>[57]</sup>, and provoke the innate immune system and exacerbate inflammation<sup>[58]</sup>.

At the same time, it merits attention that inflammatory dysregulation also participates in the progression of AMD<sup>[47,59]</sup>. Considering that pro-inflammatory cytokines, key mediators of the retinal pigment epithelium pathophysiological disorders<sup>[60]</sup>, are engaged in the control of retinal degeneration, especially macula, it is reasonable to hypothesize that OPPs-mediated secretion of inflammatory mediators may be crucial for the development of AMD<sup>[61]</sup>. On the foundation of *in vitro*, *in vivo* experiments and clinical evidences, OPPs, such as CPF and malathion, upregulated pro-inflammatory cytokine markers [e.g., interleukin (IL)-1 $\beta$ , IL-6, tumor necrosis factor (TNF)- $\alpha$  and interferon (IFN)- $\gamma$ ] both in the serum concentrations<sup>[62-64]</sup> and in target tissue expressions, including the liver<sup>[65]</sup>, kidney<sup>[65]</sup>, heart<sup>[63]</sup>, lung<sup>[66]</sup>, nerves<sup>[43,62]</sup>, testis<sup>[54]</sup>, and ocular tissues<sup>[55,64]</sup>. These effects mediated immunomodulatory activity, compromised immunocompetence, and ultimately heightened susceptibility to diseases<sup>[61]</sup>. Therefore, these findings discussed above suggest that inflammation may play a mediating role in the pathogenesis of AMD induced by OPPs exposure.

Nevertheless, there are several limitations to this analysis. First, although this study was based on the large and nationally representative samples from NHANES, the nature of cross-sectional design and observational research did not allow us to determine the temporal sequence of AMD occurrence and OPPs exposure and to establish the causal relationships between urinary DAP metabolites and AMD. Hence, there is a need for longitudinal data to confirm causality between exposure to OPPs and AMD risk. Second, despite urinary DAP metabolites as common biomarkers of OPPs exposure, they are non-specific and reflect exposure to the mixture of OPPs with similar structures, it is impossible to distinguish the specific pesticide need to be restricted for daily use. In addition, urinary DAP metabolites were measured only at the single-time point, meanwhile, taking into account rapid transformation into DAP metabolites and the complexity of body's metabolism,

the findings were insufficient to fully capture the long-term effects of cumulative OPPs exposure in humans. Thus, the misclassification of the measurement approach may discount the power of the associations. Subsequent explorations are warranted to focus on developing measurements of specific biomarkers with the aim to a more profound assessment. Third, while the extensive range of demographic and clinical confounders collected from the NHANES database enabled us to account for main covariates in this investigation, the lack of direct measurements of some known environmental risk factors for AMD (gene-related factors, chronic light exposure, or dietary components, *et al.*) may arise potential biases in this survey. Secondary analyses could integrate biobank metadata to make cross-database convergence by incorporating quantifiable indicators of additional potential risk factors—outdoor occupational patterns, leisure-time sun exposure, and geographic UV index—into the model. This approach will enhance the model's explanatory power and strengthen its clinical validity<sup>[67]</sup>. Furthermore, the majority of participants included were non-Hispanic whites, indicating the presence of possible biological and environmental differences across racial and ethnic contexts. Caution is therefore advised when generalizing our findings to a wider population. Future studies should consider more diverse samples and in-depth experiments to increase the persuasiveness and elucidate underlying biological mechanisms of toxicity of OPPs exposure on ocular system. Lastly, although the performance of the RF model was satisfactory characterized with excellent noise immunity and data stability, the variety of ML models applied was still limited, as well as the category imbalance of the proportion of patients, which resulted in the general bias toward predicting the majority of the categories and a poor predictor of a minority. In early-stage environmental exposure-disease association studies, sensitivity-driven models are essential for risk signal detection. Before extending this model to real-world applications, confirmatory testing is required due to its high false positive rate. To address the imbalanced data set, Synthetic Minority Oversampling Technique may be applied during model training to generate synthetic AMD cases, thereby improving minority class representation. Therefore, further validation analyses through external cohorts are necessary to improve the generalizability and better correct for bias mentioned above.

To the best of our knowledge, this is the first attempt to conduct a large-scale epidemiologic investigation on general population to examine the relationship between OPPs exposure and AMD risk, yielding a novel insight into the link between environmental factors and health outcomes. Since the utilization of OPPs as a substantial number of crop-specific agricultural pesticides<sup>[68]</sup>, the influence on AMD is worth

to continuously biomonitoring with the help of advanced techniques to accurately predict disease risk. Despite the good predictive results presented through ML model and various interpretable methods, this is an exploratory study and further well-designed prospective cohort researches on diverse populations are warranted to validate the clinical applicability.

#### ACKNOWLEDGEMENTS

**Authors' Contributions:** All authors contributed to the study conception and design. Material preparation, data collection and analysis were performed by Jiang YX and Gui SY. The first draft of the manuscript was written by Jiang YX and revised by Sun XD. All authors approved the final manuscript.

**Data Availability:** The datasets used and analyzed during the current study available from the corresponding author on reasonable request.

**Foundations:** Supported by the National Key Research and Development Program of China (No.2022YFC2502800); the National Natural Science Foundation of China (No.82171076); the Shanghai Municipal Education Commission (No.2023KJ05-67).

**Conflicts of Interest:** Jiang YX, None; Gui SY, None; Sun XD, None.

#### REFERENCES

- Guymer RH, Campbell TG. Age-related macular degeneration. *Lancet* 2023;401(10386):1459-1472.
- Fleckenstein M, Schmitz-Valckenberg S, Chakravarthy U. Age-related macular degeneration: a review. *JAMA* 2024;331(2):147-157.
- Rakoczy EP. The promise of long-term treatment for neovascular age-related macular degeneration. *Lancet* 2024;403(10436):1517-1519.
- Park SJ, Lee JH, Woo SJ, et al. Five heavy metallic elements and age-related macular degeneration: Korean National Health and Nutrition Examination Survey, 2008-2011. *Ophthalmology* 2015;122(1):129-137.
- Liu L, Li C, Yu HH, et al. A critical review on air pollutant exposure and age-related macular degeneration. *Sci Total Environ* 2022;840:156717.
- Brodzka S, Baszyński J, Rektor K, et al. Immunogenetic and environmental factors in age-related macular disease. *Int J Mol Sci* 2024;25(12):6567.
- Costa LG. Organophosphorus compounds at 80: some old and new issues. *Toxicol Sci* 2018;162(1):24-35.
- Nandi NK, Vyas A, Akhtar MJ, et al. The growing concern of chlorpyrifos exposures on human and environmental health. *Pestic Biochem Physiol* 2022;185:105138.
- Li AJ, Kannan K. Profiles of urinary neonicotinoids and dialkylphosphates in populations in nine countries. *Environ Int* 2020;145:106120.
- Sun HB, Sun ML, Barr DB. Exposure to organophosphorus insecticides and increased risks of health and cancer in US women. *Environ Toxicol Pharmacol* 2020;80:103474.
- Narayan S, Liew Z, Bronstein JM, et al. Occupational pesticide use and Parkinson's disease in the Parkinson Environment Gene (PEG) study. *Environ Int* 2017;107:266-273.
- Wu YD, Song J, Zhang Q, et al. Association between organophosphorus pesticide exposure and depression risk in adults: a cross-sectional study with NHANES data. *Environ Pollut* 2023;316(Pt 1):120445.
- Han L, Wang Q. Association between organophosphorus insecticides exposure and the prevalence of sleep problems in the US adults: an analysis based on the NHANES 2007-2018. *Ecotoxicol Environ Saf* 2023;255:114803.
- Guo XW, Wang H, Song QX, et al. Association between exposure to organophosphorus pesticides and the risk of diabetes among US Adults: Cross-sectional findings from the National Health and Nutrition Examination Survey. *Chemosphere* 2022;301:134471.
- Dong YQ, Xu W, Liu SP, et al. Serum albumin and liver dysfunction mediate the associations between organophosphorus pesticide exposure and hypertension among US adults. *Sci Total Environ* 2024;948:174748.
- Zhang YQ, Wu WK, Zhu XD, et al. Organophosphorus insecticides exposure and sex hormones in general U.S. population: a cross-sectional study. *Environ Res* 2022;215(Pt 2):114384.
- Dantzer J, Wood R, Buckley JP. Organophosphate pesticide exposure and atopic disease in NHANES 2005-2006. *J Allergy Clin Immunol Pract* 2021;9(4):1719-1722.e3.
- Misra UK, Nag D, Misra NK, et al. Macular degeneration associated with chronic pesticide exposure. *Lancet* 1982;319(8266):288.
- Misra UK, Nag D, Misra NK, et al. Some observations on the macula of pesticide workers. *Hum Toxicol* 1985;4(2):135-145.
- Pham H, Lingao MD, Ganesh A, et al. Organophosphate retinopathy. *Oman J Ophthalmol* 2016;9(1):49-51.
- Dahanayake P, Dassanayake TL, Pathirage M, et al. Dysfunction in macula, retinal pigment epithelium and post retinal pathway in acute organophosphorus poisoning. *Clin Toxicol (Phila)* 2021;59(2):111-117.
- Montgomery MP, Postel E, Umbach DM, et al. Pesticide use and age-related macular degeneration in the agricultural health study. *Environ Health Perspect* 2017;125(7):077013.
- Jia XL, Wang T, Zhu H. Advancing computational toxicology by interpretable machine learning. *Environ Sci Technol* 2023;57(46):17690-17706.
- Zhang GY, Fu DJ, Liefers B, et al. Clinically relevant deep learning for detection and quantification of geographic atrophy from optical coherence tomography: a model development and external validation study. *Lancet Digit Health* 2021;3(10):e665-e675.
- Dow ER, Keenan TDL, Lad EM, et al. From data to deployment the collaborative community on ophthalmic imaging roadmap for artificial intelligence in age-related macular degeneration. *Ophthalmology* 2022;129(5):e43-e59.
- Ajana S, Cougnard-Grégoire A, Colijn JM, et al. Predicting progression to advanced age-related macular degeneration from clinical, genetic, and lifestyle factors using machine learning. *Ophthalmology* 2021;128(4):587-597.
- Li SJ, Qiu YC, Li YZ, et al. Serum metabolite biomarkers for the early

- diagnosis and monitoring of age-related macular degeneration. *J Adv Res* 2024.
- 28 Gao X, Liu C, Yin LK, *et al.* Machine learning model for age-related macular degeneration based on heavy metals: The National Health and Nutrition Examination Survey 2005 to 2008. *Sci Rep* 2024;14(1):26913.
- 29 Zhang ZC, Xu B, Xu WM, *et al.* Machine learning combined with the PMF model reveal the synergistic effects of sources and meteorological factors on PM<sub>2.5</sub> pollution. *Environ Res* 2022;212(Pt B):113322.
- 30 Yu QY, Ji WJ, Prihodko L, *et al.* Study becomes insight: Ecological learning from machine learning. *Methods Ecol Evol* 2021;12(11):2117-2128.
- 31 Apley DW, Zhu JY. Visualizing the effects of predictor variables in black box supervised learning models. *Journal of the Royal Statistical Society Series B-Statistical Methodology* 2020;82(4):1059-1086.
- 32 Chen HR, Wang M, Li J. Exploring the association between two groups of metals with potentially opposing renal effects and renal function in middle-aged and older adults: Evidence from an explainable machine learning method. *Ecotoxicol Environ Saf* 2024;269:115812.
- 33 Cox LA. What is an exposure-response curve *Glob Epidemiol* 2023;6:100114.
- 34 Ribeiro MT, Singh S, Guestrin C. "Why should I trust you ": explaining the predictions of any classifier. *Proceedings of the 22nd ACM SIGKDD International Conference on Knowledge Discovery and Data Mining*. San Francisco California USA. ACM, 2016:1135-1144.
- 35 Lundberg SM, Lee SI. A unified approach to interpreting model predictions. In *Proceedings of the Proceedings of the 31st International Conference on Neural Information Processing Systems*, Long Beach, California, USA, 2017;4768-4777.
- 36 Nishihama Y, Nakayama SF, Isobe T, *et al.* Urinary metabolites of organophosphate pesticides among pregnant women participating in the Japan environment and children's study (JECS). *Int J Environ Res Public Health* 2021;18(11):5929.
- 37 Liu HR, Li RY, Zhang Y, *et al.* Economic evaluation of combined population-based screening for multiple blindness-causing eye diseases in China: a cost-effectiveness analysis. *Lancet Glob Health* 2023;11(3):e456-e465.
- 38 Gorman BR, Voloudakis G, Igo RP, *et al.* Genome-wide association analyses identify distinct genetic architectures for age-related macular degeneration across ancestries. *Nat Genet* 2024;56(12):2659-2671.
- 39 Stevens DR, Blaauwendraad SM, Bommarito PA, *et al.* Gestational organophosphate pesticide exposure and childhood cardiovascular outcomes. *Environ Int* 2024;193:109082.
- 40 Teodoro M, Briguglio G, Fenga C, *et al.* Genetic polymorphisms as determinants of pesticide toxicity: Recent advances. *Toxicol Rep* 2019;6:564-570.
- 41 Darney K, Kasteel EEJ, Buratti FM, *et al.* Bayesian meta-analysis of inter-phenotypic differences in human serum paraoxonase-1 activity for chemical risk assessment. *Environ Int* 2020;138:105609.
- 42 Zúñiga-Venegas L, Pancetti FC. DNA damage in a Chilean population exposed to pesticides and its association with PON1 (Q192R and L55M) susceptibility biomarker. *Environ Mol Mutagen* 2022;63(4):215-226.
- 43 Mostafalou S, Abdollahi M. The susceptibility of humans to neurodegenerative and neurodevelopmental toxicities caused by organophosphorus pesticides. *Arch Toxicol* 2023;97(12):3037-3060.
- 44 Kahl VFS, da Silva FR, da Silva Alves J, *et al.* Role of PON1, SOD2, OGG1, XRCC1, and XRCC4 polymorphisms on modulation of DNA damage in workers occupationally exposed to pesticides. *Ecotoxicol Environ Saf* 2018;159:164-171.
- 45 Söğüt E, Ortak H, Aydoğan L, *et al.* Association of paraoxonase 1 L55M and Q192R single-nucleotide polymorphisms with age-related macular degeneration. *Retina* 2013;33(9):1836-1842.
- 46 Javadzadeh A, Ghorbanihaghjo A, Bahreini E, *et al.* Serum paraoxonase phenotype distribution in exudative age-related macular degeneration and its relationship to homocysteine and oxidized low-density lipoprotein. *Retina* 2012;32(4):658-666.
- 47 Fleckenstein M, Keenan TDL, Guymer RH, *et al.* Age-related macular degeneration. *Nat Rev Dis Primers* 2021;7(1):31.
- 48 Jia LH, Dong YD, Yang HM, *et al.* Serum superoxide dismutase and malondialdehyde levels in a group of Chinese patients with age-related macular degeneration. *Aging Clin Exp Res* 2011;23(4):264-267.
- 49 García-Quintanilla L, Rodríguez-Martínez L, Bandín-Vilar E, *et al.* Recent advances in proteomics-based approaches to studying age-related macular degeneration: a systematic review. *Int J Mol Sci* 2022;23(23):14759.
- 50 Kushwah N, Bora K, Maurya M, *et al.* Oxidative stress and antioxidants in age-related macular degeneration. *Antioxidants (Basel)* 2023;12(7):1379.
- 51 Yu F, Wang ZR, Ju B, *et al.* Apoptotic effect of organophosphorus insecticide chlorpyrifos on mouse retina *in vivo* via oxidative stress and protection of combination of vitamins C and E. *Exp Toxicol Pathol* 2008;59(6):415-423.
- 52 Bai J, Deng SW, Fu HY, *et al.* Chlorpyrifos induces placental oxidative stress and barrier dysfunction by inducing mitochondrial apoptosis through the ERK/MAPK signaling pathway: *in vitro* and *in vivo* studies. *Sci Total Environ* 2023;903:166449.
- 53 Gomathy N, Sumantran VN, Shabna A, *et al.* Tolerance of ARPE 19 cells to organophosphorus pesticide chlorpyrifos is limited to concentration and time of exposure. *Pestic Biochem Physiol* 2015;117:24-30.
- 54 Alipanah H, Kabi Doraghi H, Sayadi M, *et al.* Subacute toxicity of chlorpyrifos on histopathological damages, antioxidant activity, and pro-inflammatory cytokines in the rat model. *Environ Toxicol* 2022;37(4):880-888.
- 55 AlKahtane AA, Ghanem E, Bungau SG, *et al.* Carnosic acid alleviates chlorpyrifos-induced oxidative stress and inflammation in mice cerebral and ocular tissues. *Environ Sci Pollut Res Int* 2020;27(11):11663-11670.

- 56 Geller AM, Sutton LD, Marshall RS, *et al.* Repeated spike exposure to the insecticide chlorpyrifos interferes with the recovery of visual sensitivity in rats. *Doc Ophthalmol* 2005;110(1):79-90.
- 57 Hernandez-Cortes D, Alvarado-Cruz I, Solís-Heredia MJ, *et al.* Epigenetic modulation of Nrf2 and Ogg1 gene expression in testicular germ cells by methyl parathion exposure. *Toxicol Appl Pharmacol* 2018;346:19-27.
- 58 Potilinski MC, Tate PS, Lorenc VE, *et al.* New insights into oxidative stress and immune mechanisms involved in age-related macular degeneration tackled by novel therapies. *Neuropharmacology* 2021;188:108513.
- 59 Ambati J, Atkinson JP, Gelfand BD. Immunology of age-related macular degeneration. *Nat Rev Immunol* 2013;13(6):438-451.
- 60 Hansman DS, Du JH, Casson RJ, *et al.* Eye on the horizon: the metabolic landscape of the RPE in aging and disease. *Prog Retin Eye Res* 2025;104:101306.
- 61 Camacho-Pérez MR, Covantes-Rosales CE, Toledo-Ibarra GA, *et al.* Organophosphorus pesticides as modulating substances of inflammation through the cholinergic pathway. *Int J Mol Sci* 2022;23(9):4523.
- 62 Weis GCC, Assmann CE, Mostardeiro VB, *et al.* Chlorpyrifos pesticide promotes oxidative stress and increases inflammatory states in BV-2 microglial cells: a role in neuroinflammation. *Chemosphere* 2021;278:130417.
- 63 Alruhaimi RS. Betulinic acid protects against cardiotoxicity of the organophosphorus pesticide chlorpyrifos by suppressing oxidative stress, inflammation, and apoptosis in rats. *Environ Sci Pollut Res Int* 2023;30(17):51180-51190.
- 64 Alanazi IS, Altyar AE, Zaazouee MS, *et al.* Effect of moringa seed extract in chlorpyrifos-induced cerebral and ocular toxicity in mice. *Front Vet Sci* 2024;11:1381428.
- 65 Ismail AA, Hendy O, Abdel Rasoul G, *et al.* Acute and cumulative effects of repeated exposure to chlorpyrifos on the liver and kidney function among Egyptian adolescents. *Toxics* 2021;9(6):137.
- 66 Aitken AV, Minassa VS, Batista TJ, *et al.* Acute poisoning by chlorpyrifos differentially impacts survival and cardiorespiratory function in normotensive and hypertensive rats. *Chem Biol Interact* 2024;387:110821.
- 67 Wang Y, Du R, Xie S, *et al.* Machine learning models for predicting long-term visual acuity in highly myopic eyes. *JAMA Ophthalmol* 2023;141(12):1117-1124.
- 68 Clune AL, Ryan PB, Barr DB. Have regulatory efforts to reduce organophosphorus insecticide exposures been effective. *Environ Health Perspect* 2012;120(4):521-525.